

Research Article

Mechanism Study on Elevation Effect of Blast Wave Propagation in High Side Wall of Deep Underground Powerhouse

Xinping Li ¹, Junlin Lv ², Yi Luo ¹ and Tingting Liu ¹

¹Hubei Key Laboratory of Roadway Bridge and Structure Engineering, Wuhan University of Technology, No. 122 Luoshi Rd., Wuhan 430070, China

²School of Civil Engineering and Architecture, Wuhan University of Technology, No. 122 Luoshi Rd., Wuhan 430070, China

Correspondence should be addressed to Xinping Li; xinpingli@whut.edu.cn

Received 20 June 2018; Accepted 12 September 2018; Published 14 November 2018

Academic Editor: Lutz Auersch

Copyright © 2018 Xinping Li et al. This is an open access article distributed under the Creative Commons Attribution License, which permits unrestricted use, distribution, and reproduction in any medium, provided the original work is properly cited.

In view of the influence of blasting excavation in the deep burial underground powerhouse on the dynamic disturbance and blasting vibration of side wall and surrounding rock, the blasting vibration test method is often used for on-site monitoring and control. Taking the blasting excavation of the high side wall of an underground powerhouse of a hydropower station as the engineering background, a long-term blasting vibration test is carried out on the site. The measuring points are arranged along the elevation direction and horizontal direction of the high side wall of the powerhouse. Through analyzing and comparing the blasting vibration velocity values extracted from a large number of on-site measured data in the elevation direction, an interesting phenomenon is found. The measured vibration velocity of the rock anchor beam in the area far away from the blasting is greater than that in the area near the blasting, and the vibration velocity after the casting of the rock anchor beam is greater than that before the casting. In order to avoid the randomness and contingency of the measured data, based on the blasting parameters, loading quantity, and rock mechanical characteristics used in the field, the elevation effect of the numerical model of the underground powerhouse is established by using the dynamic finite element software. By comparing the numerical simulation and the on-site monitoring of the elevation direction vibration velocity at the same location, it is found that the two have the same law, which verifies the reliability of the numerical calculation model. By changing the elevation and horizontal distances to select the measuring points in the numerical model, the propagation curve of the blasting vibration of the high side wall of the underground powerhouse in the elevation direction is obtained and the wave propagation phenomenon and the local elevation amplification effect of blasting vibration velocity in the side wall of the powerhouse are found. By means of changing the morphology characteristics of the rock anchor beam, a numerical calculation model of the rock anchor beam before casting is established, and the blasting vibration velocity in the elevation direction of the same measuring point as the original model is extracted. The analysis and comparison results show that the “whiplash effects” caused by the reflection superposition of the convex morphology characteristics of the rock anchor beam on the blast wave and the vibration response of the rock mass at the step part is the main factor for the elevation effect. The fluctuation phenomenon of the vibration velocity in the elevation direction is caused by the natural frequency and the main vibration mode of the high side walls, and the reflection superposition of the convex geomorphology characteristics of the rock anchor beam will aggravate this fluctuation phenomenon. Therefore, in the construction of deep underground powerhouses, attention should be paid to the blasting construction and support design of the rock anchor beam.

1. Introduction

In recent years, China has built and developed a number of giant hydropower projects with installed capacity of more than three million kilowatts in the Jinshajiang, Yalongjiang, and Dadu river basins in the west [1]. With the advancement of hydropower development, the buried depth of underground

powerhouses of hydropower stations in China has also been continuously updated. For example, (1) the Dagangshan Hydropower Station is one of the major hydropower projects recently developed in the main stream of Dadu River. The vertical depth of the underground powerhouse is 390 m–520 m, and the horizontal depth is 310 m–530 m. (2) The longest tunnel section of the diversion project in the central

region of the Yunnan province is 55 km long, the maximum depth is 1370 m, and the self-gravity stress is about 37 MPa. (3) The maximum depth of the Hongliangzi Tunnel at the Wudongde Hydropower Station in Jinsha River is 2300 m. The large-scale deep rock mass excavation will inevitably face the problems of high ground stress and strong excavation disturbance [2]. The design and construction of underground cavern groups with large section, long tunnel, large depth, and high side wall have increased the difficulty of excavation for blasting excavation construction [3].

In the process of blasting excavation of underground powerhouse of the hydropower station, when the vibration caused by blasting reaches enough strength, various failure phenomena occurs [4–6]. In areas with elevation changes, it is a very important research content to study the elevation amplification effect of blasting vibration. Many domestic and foreign scholars have studied the elevation effect and found that the blast stress wave will appear with a certain degree of amplification in the process of propagation in the elevation direction, which is usually called the elevation amplification effect [7–9]. Havenith et al. [10] used the two- and three-dimensional finite element methods to analyze the Ananevo rockslide slope and found that, in the low-velocity zone of the rock surface, there is a great relationship between the amplification of the vibration wave and the localization of the strain, especially in the surface where there are prominent parts. Marrara and Suhadolc [11] used the blasting instead of the seismic source to analyze the vibration amplification effect. The results showed that the characteristics and depth of the blasting source and the distances of the measuring points will lead to different excitations. When the frequency is greater than 2 Hz, the amplification effect in the monitoring area is obvious. Graizer [12] believed that the low-velocity zone and geological landform are the main reasons for the vibration amplification effect. Guo et al. [13] proposed that the elevation amplification effect is a slope effect phenomenon, and the size of the slope effect is related to the position of the measuring point relative to the slope surface and the condition of the slope surface itself. Jiang et al. [14] used numerical model calculations to show that, for the monitoring point on the same side slope, along with the increase of horizontal distance and elevation difference, the blasting vibration velocity is dominated by the attenuation trend. At the same level, the blasting vibration velocity decreases with the increase of the slope gradient, but there is a dominant phenomenon of elevation magnification effect. Tang et al. [15, 16] obtained the blasting vibration formula reflecting the positive elevation difference amplification effect by using the dimension analysis method. Combined with the negative excavation vibration monitoring of the foundation blasting in the second phase of the Guangdong Lingao nuclear power station, it is pointed out that the concave geomorphology has an attenuation effect on blasting vibration waves. Convex geomorphology has amplification effect on the blasting vibration wave, and it decreases with the increase of blasting source distance. A blasting vibration formula that can reflect the positive elevation amplification effect is obtained through dimension analysis.

The mechanism of elevation effect produced by scholars at home and abroad has mainly formed the following three theories. (1) The first theory is the action mechanism of the seismic wave of the positive elevation difference terrain. Zhou Tongling [17] believed that the magnification effect of positive elevation difference terrain is mainly due to the influence of the interface group. When the impedance of the stratum decreases from the deep layer to the surface layer, the vibration velocity of the particle caused by refracted wave is $v_z > v_l$. According to the superposition characteristics of the refracted wave of the interface group, v_z increases with the increase of height difference H . (2) The second theory is “whiplash effect” of the rock slope. Chen et al. [18] believed that the step part of the rock slope is equivalent to the prominent part of the main structure. The natural vibration frequency of this part is within the main frequency range of the blasting vibration load, so the blasting vibration at the step part will produce a “whiplash effect,” and the rock mass vibration velocity at the edge is larger. (3) The third theory is ray theory of slope elevation amplification effect. Shi et al. [19] believed that the slope elevation amplification effect is due to the reflection superposition of slope surface. Time delays of different wave fields reaching the particle are different, which results in a rhythmic change of the elevation amplification effect in the slope. Under the action of low-frequency waves, the elevation amplification factor is sparse and rhythmical. The higher the incidence frequency is, the more obvious the rhythm is and the more extreme the points are. The slope lithology and slope gradient are the main factors that affect the elevation magnification effect of the slope.

According to the above studies on the elevation amplification effect and its mechanism at home and abroad, it can be found that the research object is mainly concentrated on the elevation effect of the rock slope [20, 21]. For the high side wall structures of underground chambers and deep underground powerhouses, there is no systematic and in-depth study on their elevation effects. Based on the basic mechanical properties of rock mass, actual blasting parameters and the monitoring data of blasting vibration in the elevation direction of the side wall in the process of blasting excavation of the underground powerhouse of the Baihetan Hydropower Station in China, the propagation law of blast wave in the elevation direction of the deep buried underground powerhouse is obtained through the analysis of the measured data. The dynamic finite element method is used to simulate and calculate the blasting vibration velocity of rock mass in the elevation direction, and it is verified, refined, and expanded by comparison with the vibration velocity of actual measuring point in the field. Then, using the rock anchor beam as the key part and changing its geomorphological characteristics to restore the shape of the rock anchor beam before casting, a new numerical model was established. By comparing the numerical results of the two models, the blast wave propagation characteristics at this part and the mechanism of the elevation effect are found out so as to provide guiding suggestions for the blasting construction and stability control of the rock anchor beam (Figure 1).

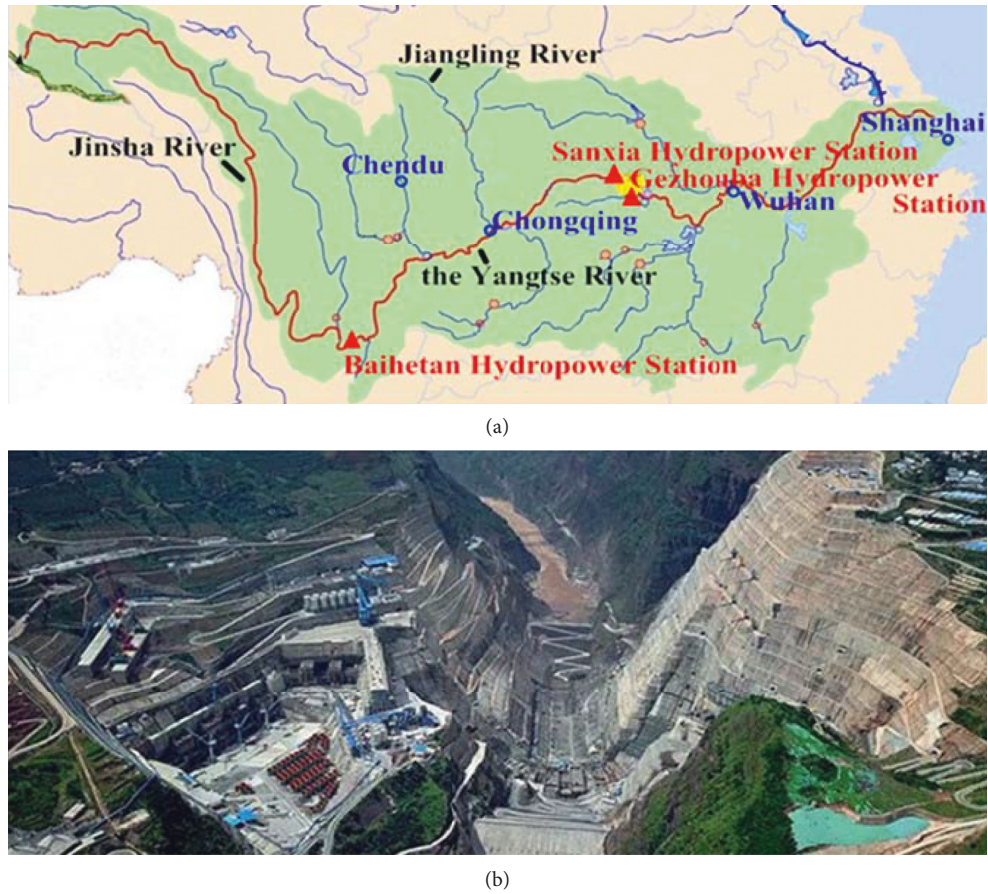


FIGURE 1: Aerial view (a) and location map (b) of the Baihetan Hydropower Station.

2. Test

2.1. Engineering Background. The normal storage level of the Baihetan Hydropower Station after construction is 825 m, with a capacity of $2.06 \times 10^9 \text{ m}^3$ and a preliminary installed capacity of 16 million kW. The power generating set of the hydropower station is set in the underground powerhouse, with eight sets of one million kW hydroelectric generating sets on both sides, which will be the second largest hydropower station in China next to the Three Gorges hydropower station and the largest underground hydropower project in the world [22]. The main building design dimensions are $439 \text{ m} \times 32.2 \text{ m} \times 78.5 \text{ m}$ (length \times width \times height), which reached the world's largest underground powerhouse; the maximum span of the top arch excavation is 15 m, and the excavation height is approximately 84.1 m. The buried depths of the powerhouse on the left and right bank are 350 m and 550 m, respectively. The excavation volume of the deep rock mass in the underground cavern group exceeds 25 million m^3 , the total length of the underground cavern group is 217 km, the span of the main powerhouse is 32.2 m, and the length is 439 m, all of which are the first in the world [23, 24]. The difficulty of excavation technology of the underground powerhouse project which has a large span, a large depth of burial, and a complex geological structure is the highest among the hydropower projects in the world.

2.2. Blasting Vibration Test. In order to control the impact of blasting vibrations, blasting vibration test methods are often used in the field [25, 26]. According to the field and actual conditions, the blasting vibration test is carried out in the main powerhouse of the hydropower station. The diameter of the blasting hole is of 90 mm, the depth is 4~6.2 m, the hole distance of the main blasting hole is 2 m to 3 m, and the row distance is 2 m to 3 m. The blast hole uses $\varnothing 70 \text{ mm}$ emulsion explosives for continuous charge, and the single hole dosage is timely adjusted according to the blasting conditions, mainly between 10 kg and 26 kg. The test system for the blasting vibration test is a L20 vibration recorder manufactured by Chengdu Jiaobo Technology Co., Ltd. In order to study the propagation law of the blast stress wave in the elevation direction, ten measuring points are arranged at each test, the vibration velocity sensors of each test point are arranged on the same elevation line, and two columns are arranged in the horizontal direction. For the determination of the elevation distance, the sensor in the lowest place is arranged at the bottom of the powerhouse and the distance between two sensors in the center is 5 m, and two points are set at the rock anchor beam and the upper part of 3 m. Each column has five elevation measuring points, and two columns have a total of ten measuring points. The field test point layout is shown in Figure 2 in MP1~MP10, and the structure and size of the powerhouse are shown in Figure 3. The test results of the blasting vibration in the elevation

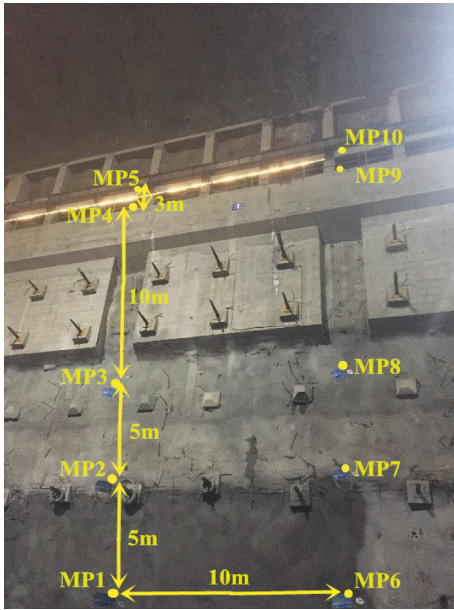


FIGURE 2: Instrument layout for the blasting vibration test of high side wall of the powerhouse.

direction in the main powerhouse are shown in Table 1. V_x represents the vibration velocity parallel to the direction of the side wall, V_y represents the vibration velocity perpendicular to the side wall direction, and V_z represents the particle vibration velocity in the elevation direction. Due to the study of the elevation effect, the blast wave propagates in the z direction, and the direction of the vibration is the motion direction of the particle phase, i.e., the y direction. Therefore, the research should focus on the vibration velocity value of the measured data in the y direction. An interesting phenomenon can be found by analyzing and comparing a large number of field measured vibration velocity V_y . The measured vibration velocity of the rock anchor beam in the area far away from the blasting is greater than that in the area near the blasting, and the vibration velocity after the casting of the rock anchor beam is greater than that before the casting, as shown in Table 1.

3. Numerical Model Calculation of Elevation Effect in Underground Powerhouse

3.1. Parameter Calculation of Numerical Model. The measured and inverse analysis shows that the maximum principal stress at the location of the underground cavern group on the right bank of the Baihetan Hydropower Station is 21.5 MPa [27]. According to the current related industry classification criteria, the ground stress at the location of the main transformer tunnel is greater than 20 MPa, which belongs to the high ground stress area. According to the research situation in the literature [27], the vertical ground stress is about 10.3 MPa, which is calculated according to the burial depth of the cavern. Since the horizontal measured principal stress is $\sigma_1 = 21.5$ MPa and $\sigma_3 = 10.3$ MPa, according to the stress analysis formula of the plane stress

state in elasticity mechanics, it can be found that the horizontal stress in the axial direction of the cavern is 21.35 MPa, and the horizontal stress perpendicular to the axial direction of the cavern is 10.45 MPa. According to the principle of force balance, the peak pressure of the shock wave applied to the blast hole wall is equivalently applied to the core line of the holes [28]. After the blasting load is approximately equivalent, it acts on the plane determined by the center line of the blasting hole of the same row and the hole axis, so the method of applying the blasting load is the equivalent load. The total time of the blasting pressure is 10 ms, with a positive pressure rise time of 2.3 ms and a descending time of 7.7 ms. When numerical simulations are used to analyze the dynamic response of rock mass subjected to blast impact loading, according to the study [29], the results of dynamic response of rock mass blasting in the kinematic hardening model is closer to those in the actual project, which can more accurately reflect the dynamic response characteristics of surrounding rock under explosion. Therefore, the constitutive model adopted in the numerical model is the kinematic hardening model.

3.2. Three-Dimensional Numerical Model of Elevation Effect in Underground Powerhouse. Based on the actual blasting excavation of the main powerhouse of the Baihetan Hydropower Station, the single side of the high side wall and the upper vault structure are selected as the finite element simulation objects, and the finite element calculation model is established by the ANSYS/LS-DYNA dynamic finite element software [30, 31]. The model is selected in the middle part of the actual part of the main powerhouse, and the size of the model is selected according to the actual construction design drawing (Figure 3). The span of the powerhouse is selected by half of the actual value, the span of the baseboard is 15.5 m, the span of the upper spandrel is 17 m, the height of the model is chosen as the actual value, and the height from the actual excavation baseboard to the vault is 42 m. To avoid boundary effects on the calculation results, the length, width, and thickness of the model take 160 m, 50 m, and 35 m, respectively, as shown in Figure 4(a). In order to deeply and systematically study the elevation effect of the blasting vibration of the side wall of an underground powerhouse, the actual excavation process is used as the basis for simulating the blasting excavation process in the baseboard of the plant model. In order to ensure the reliability of the simulation results, in the same conditions of the bottom elevation, taking 5 m as the footage of the blasting cycle, it is proceeding forward in the positive direction along the Z -axis in 5 times. In order to further study the relationship between elevation effect and height difference in the elevation direction, it is divided into three layers in the negative direction along the Y -axis, the excavation height of each layer is 5 m, and the excavation is carried out from the top to the bottom, as shown in Figure 4(b). The specific excavation diagram is shown in Figure 5. Therefore, a total of 15 three-dimensional models of blasting excavation for underground powerhouses have been established.

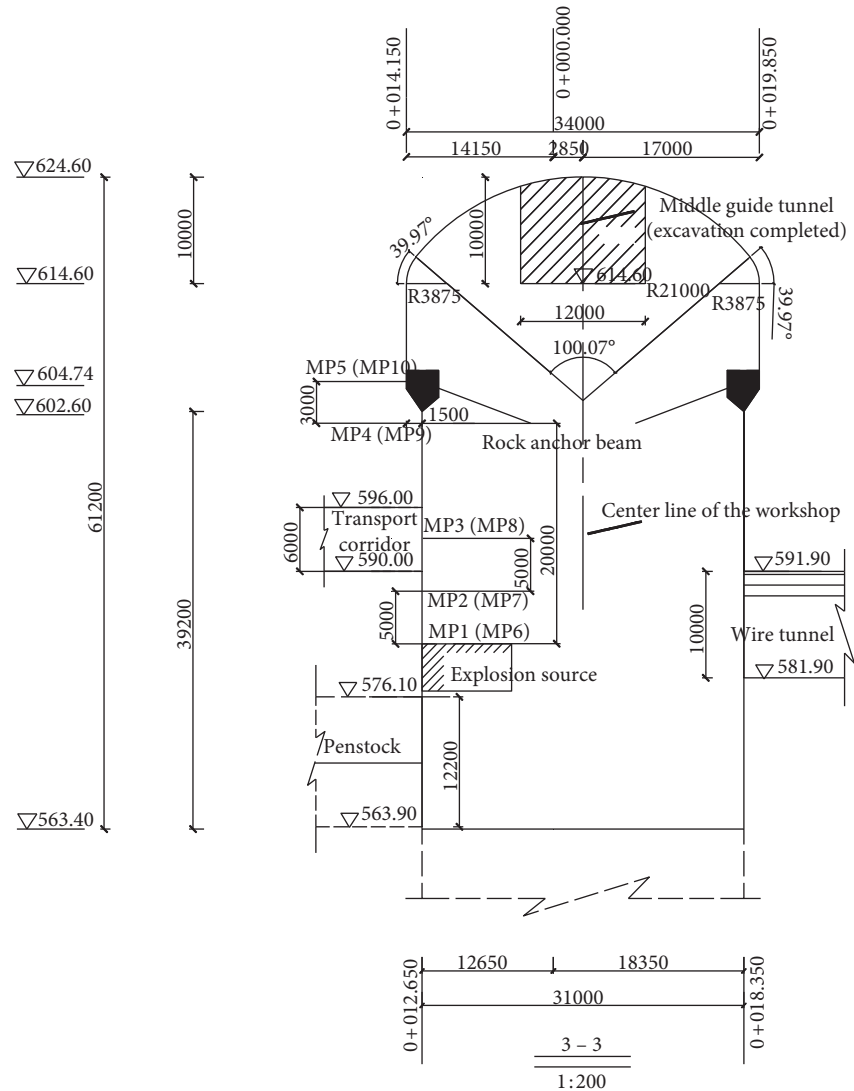


FIGURE 3: Front view and the dimensions of the underground powerhouse of the hydropower station (unit: mm).

According to the site survey data, the rock parameters of the underground cavern rock anchor beam can be obtained as shown in Table 2 [32].

3.3. Comparative Analysis between Numerical Calculation and Actual Measurement of Blasting Vibration Velocity. Based on the basic mechanical properties and actual blasting parameters of the blasting excavation at the Baihetan Hydropower Station, the numerical simulation was carried out. The blasting vibration velocity values were analyzed and calculated and compared with the measured results. In the study of rock explosion dynamics, the static analysis is carried out first, which can be used to observe and verify the rationality of the initial stress state of the rock before the application of the explosive load. It can also be seen that whether the establishment of the model and the application of boundary conditions are correct. As shown in Figure 6(a), it can be known from the stress distribution of the ground stress before

the application of the blasting load that, without considering the support conditions, the side wall of the powerhouse is a stress relaxation zone, which mainly bears tensile stress, and its value is one order of magnitude lower than the ground stress. In addition, as shown in Figure 6(b), under the action of dynamic and static combination of ground stress and blasting load, the side wall of the powerhouse is subjected to tensile stress after the application of the blasting load, and the maximum stress is increased by two orders of magnitude. The rock mass in the blasting area is subjected to pressure stress. The prestressed anchor used in the actual project is to prevent the deterioration of rock properties due to the excessive accumulation of deformation in the middle part of the side wall and the rock anchor beam and the excessive stress at the vault. The static analysis before the application of the explosive load is consistent with the theoretical analysis in the elastic mechanics and the experience in the actual engineering, which shows that the establishment of the model and the selection of the boundary conditions are reasonable.

TABLE 1: Summary of the test results of the blasting vibration in the elevation direction in the powerhouse.

Status of construction	Numbering	Quantity of explosive (kg)	Horizontal distance (m)	Elevation (m)	V_y (cm/s)	Dominant frequency (Hz)
Rock anchor beam after casting	1	26	10	0	9.91	81.2
			10	5	7.27	5.1
			10	10	5.02	44.4
			10	20	5.19	15.3
			10	23	4.8	29.9
			20	0	3.9	26.2
	2	26	20	5	3.08	126.6
			20	10	2.57	260.4
			20	20	2.71	27
			20	23	2.5	285.2
			10	0	7.23	75.7
			10	5	6.09	11.3
	3	22	10	10	5.31	167.4
			10	20	5.3	51.9
			10	23	5.2	66
			20	0	4.2	15.7
			20	5	2.16	82.2
			20	10	1.77	85.2
	4	22	20	20	1.87	42.2
			20	23	1.76	76.8
			10	0	7.06	60.4
			10	5	6.05	293
			10	10	5.0	334.8
			10	20	5.03	21.7
5	19	10	23	4.9	187.5	
		20	0	3.9	195.3	
		20	5	1.98	76.8	
		20	10	1.77	97.7	
		20	20	1.85	41.5	
		20	23	1.6	293	
Rock anchor beam before casting	7	26	10	0	9.78	71.6
			10	20	3.12	33.8
	8	26	20	0	3.94	93.8
			20	20	1.06	24.3
	9	23	10	0	6.88	176.8
			10	20	2.4	40.1
	10	23	20	0	4.12	185.2
			20	20	0.92	18.4
	11	20	10	0	6.71	74.8
			10	20	2.37	56.2
	12	20	20	0	3.72	58.6
			20	20	0.88	39.7

Through the postprocessing program, the peak vibration velocity of the measuring point in Figure 2 that is the same as the actual position is extracted and compared with the measured peak vibration velocity of the same part of the field and the calculated value of the theoretical formula, as shown in Figure 7. In the numerical model, the blast wave propagation direction corresponds to the y direction, and the vibration direction is the x direction. Since the calculation result is analyzed for the particle vibration velocity, the main research here is the change law of the vibration velocity of the x direction in the y direction propagation process. Therefore, all the values extracted in the numerical simulation results are the vibrational velocity values in the x direction. The measured data of first group are the blasting vibration velocity of the elevation measuring point at

a horizontal distance of 10 m from the blasting source in the blasting test of the underground powerhouse. In order to further improve the progress and reliability of numerical simulation data, five numerical simulation models for excavation of the first layer are taken as objects. The blasting vibration velocity values in the elevation direction of the measuring points at the same position in the blasting test are selected, and the simulation results are compared with the measured data and the theoretical calculation, as shown in Figure 7(a). The measured data of the second group are the blasting vibration velocity of the elevation measuring point at a horizontal distance of 20 m from the blasting source in the blasting test of the underground powerhouse. The numerical model also selects the blasting vibration velocity in the elevation direction of the measuring points at the same

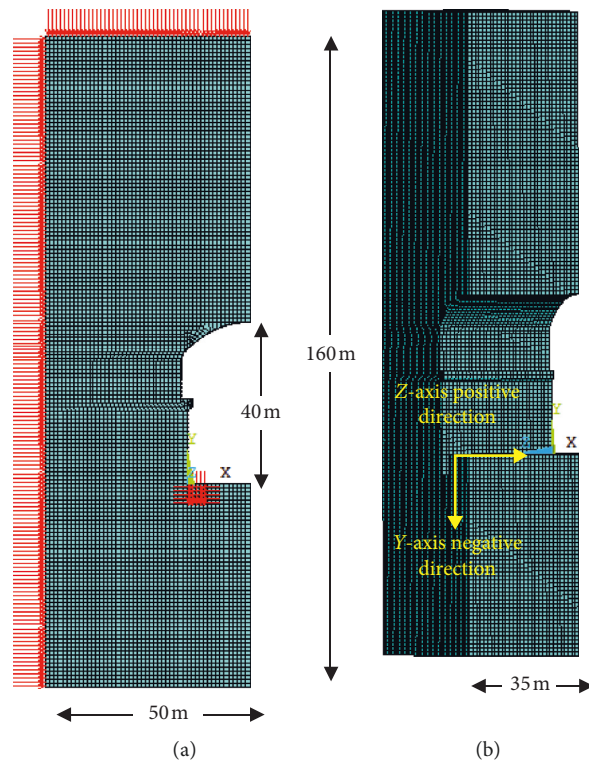


FIGURE 4: Front view and lateral view of the calculation model for blasting excavation of the rock anchor beam. (a) Front view. (b) Lateral view.

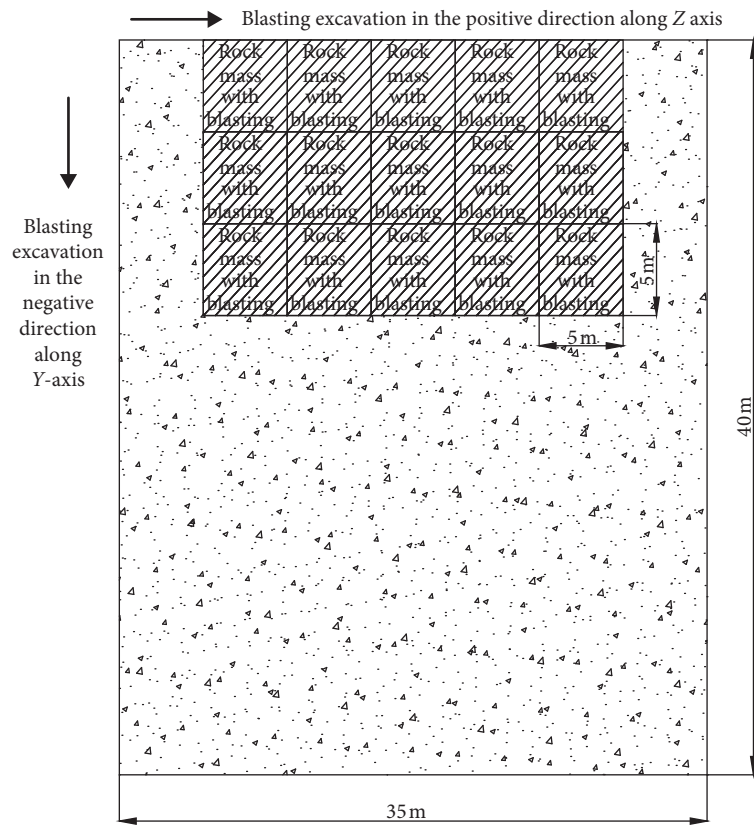


FIGURE 5: Schematic diagram of stratified partition excavation in the baseboard of the numerical model.

TABLE 2: Rock mass physical and mechanical material.

ρ (kg/m ³)	E (GPa)	μ	σ_t (MPa)	σ_c (MPa)	E_t (MPa)
2750	50.0	0.23	6.0	100.0	8.0

position in the blasting test and compares the simulation results with measured data and theoretical calculations, as shown in Figure 7(b). From the analysis and comparison results, it is found that the propagation law of blasting vibration velocity in the side wall of underground powerhouse is the same as that in the slope, which can verify the reliability of the measured data and the numerical model. It can be seen that the blasting vibration velocity is not a simple attenuation process in the elevation direction, but an amplification effect occurred in the local position.

In order to further study the propagation law of the blasting vibration velocity in the elevation direction during the excavation of underground powerhouses, a line of elevation measuring points which are directly above each simulated excavation block and with a horizontal distance of 0 m from the blasting source are selected as objects. In order to eliminate the influence of other factors on the blasting vibration velocity, the variable is only controlled to the change of elevation. The height difference of each measuring point is 1 m. In the first layer of the excavation model, each model extracts 52 measuring points. In the second layer of the excavation model, each model extracts 57 measuring points. In the third layer of the excavation model, each model extracts 62 measuring points. According to the result of the postprocessing program, the vibration velocities of the x direction of all measuring points in each model are extracted and processed into a graph. A total of fifteen numerical models of blasting excavation in three layers are grouped according to the same layer. The calculation results of the five numerical models in each group are organized into a graph and made a comparison analysis. The calculation result of the first layer is shown in Figure 8(a). The calculation result of the second layer is shown in Figure 8(b). The calculation result of the third layer is shown in Figure 8(c).

Through the calculation, analysis, and comparison of the results of Figure 8, the following can be found. (1) In the calculation of the numerical model of the powerhouse, the blasting vibration velocity in the elevation direction of the side wall shows the trend of attenuation as a whole and the blasting vibration velocity gradually decreases with the increase of the elevation. (2) In the trend of the overall attenuation, the blasting vibration velocity in the elevation direction has a sudden change point at the interval of 5 m. (3) In the first layer of the excavation model, the elevation of the rock anchor beam is 20 m. In the second layer of the excavation model, the elevation of the rock anchor beam is 25 m. In the third layer of the excavation model, the elevation of the rock anchor beam is 30 m. The curve change trend shows that the vibration velocity of the particle at the rock anchor beam is greater than that at the measuring point 5 m below the rock anchor beam and has the same local amplification effect as that of the measured data. (4) The local amplification effect gradually decreases as the elevation increases. In the excavation model, the elevation of 45 m of the first layer, the elevation of 50 m of the second layer, and

the elevation of 55 m of the third layer are located in the arch of the powerhouse, and above the elevation of the arch shoulder, the local magnification effect basically disappears.

In order to further analyze the local amplification effect and its production mechanism, the excavation process of the first model of the first layer is taken as the research object. By changing the horizontal distance from the blast source, the horizontal distances are 0 m, 5 m, 10 m, 15 m, and 20 m in the order of 5 m increments. A total of five groups of elevation measuring points are selected, and each group has a total of 52 measuring points. The blasting vibration velocity in the x direction is extracted and processed into a curve, as shown in Figure 9. The following can be found. (1) The blasting vibration velocity in the elevation direction shows an overall trend of attenuation with the increase of horizontal distance. (2) Although the value of the blasting vibration velocity in the elevation direction at different horizontal distances from the blast source is different, the location of local amplification effect and the overall law are relatively uniform. It can be seen that the effect of the horizontal distance in the blast center distance on the elevation effect is basically negligible. The elevation effect of the blasting vibration velocity in the side wall of the underground powerhouse is mainly related to the magnitude of elevation.

Taking the excavation process of the first model of the first layer as the research object, by changing the height difference, 5 m is increased at a time. The elevations are 0 m, 5 m, 10 m, 15 m, and 20 m in order to select five groups of measuring points. Each group selects 21 measuring points according to the interval of 1 m in horizontal distance. The position in which the elevation is 0 m is the baseboard of the powerhouse, and the position in which the elevation is 20 m is the rock anchor beam. The blasting vibration velocity in the elevation direction is extracted and processed into a curve, as shown in Figure 10. It has the following rules. (1) Except for the rock anchor beam, the change of elevation does not affect the trend that the blasting vibration velocity in the elevation direction decreases with the increase of the horizontal direction. However, the oscillating wave appears when the blasting vibration velocity in the elevation direction of the rock anchor beam increases along the horizontal distance, which leads to the local magnification phenomenon. (2) The blasting vibration velocity in the elevation direction of the same elevation location tends to decrease as the horizontal distance increases. However, the blasting vibration velocity of some high elevation is larger than that of low elevation, and a local elevation magnification effect appears.

According to the field blasting vibration test data and the theoretical calculation formula of slope elevation amplification effect, combined with the multiangle analysis and comparison of the above numerical simulation results, the main conclusions are drawn as follows. (1) In the propagation process of the blast stress wave along the elevation direction of the side wall of underground powerhouse, the local amplification phenomenon of wave propagation of the blasting vibration velocity in the elevation direction appears. However, with the increase of elevation, especially after exceeding the position of the spandrel, the local amplification effect gradually disappears. (2) The particle vibration velocity of the rock anchor beam has more obvious

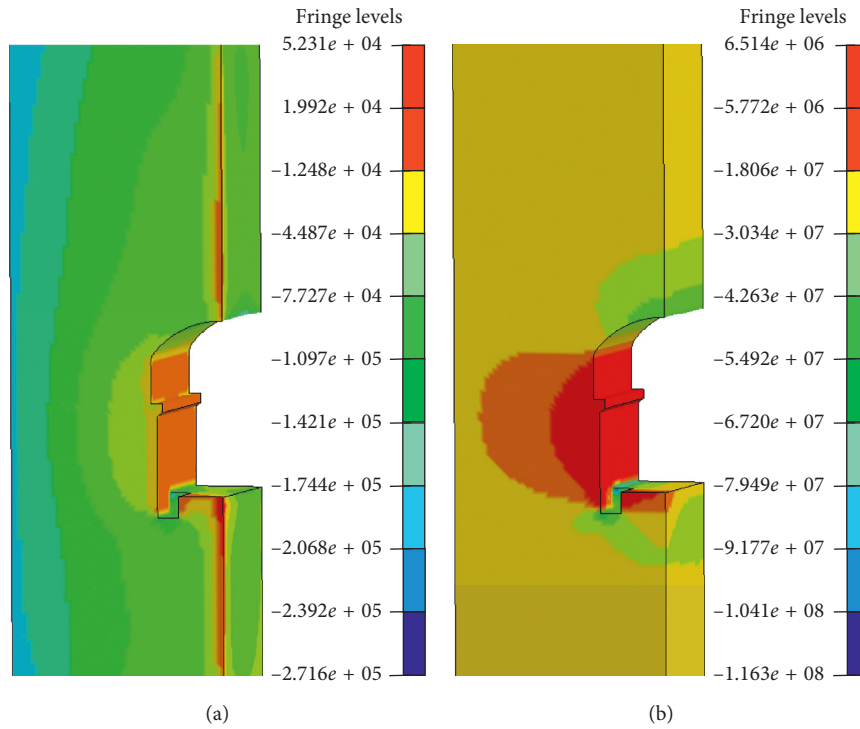


FIGURE 6: The maximum principal stress nephogram (a) before and (b) after the application of the explosive load.

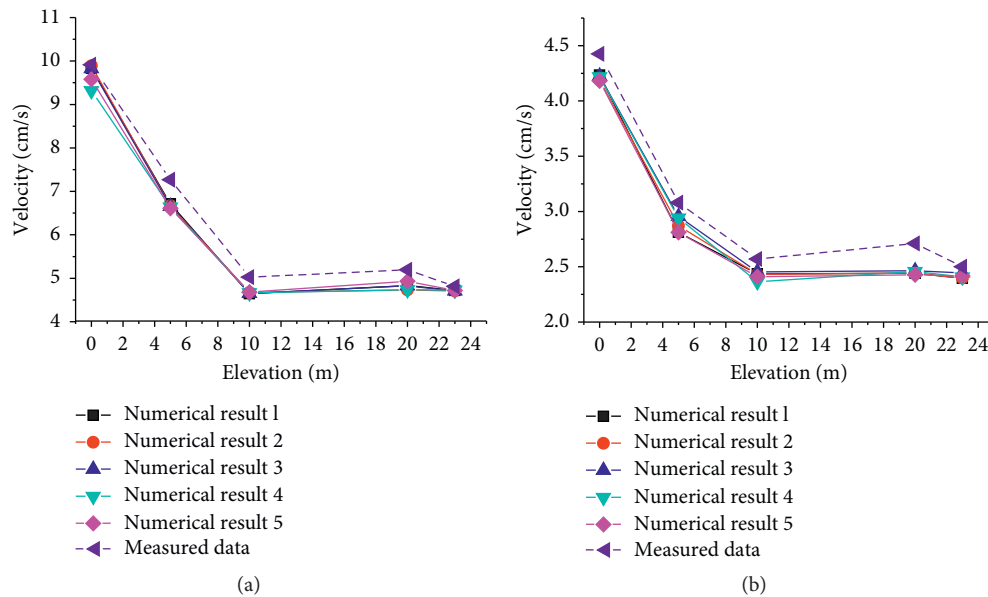


FIGURE 7: Comparison of the vibration velocity of numerical simulation in the elevation direction with the measured data and the calculated results. Horizontal distance of (a) 10 m and (b) 20 m.

amplification effect than that of other locations. After summarizing a large number of practical engineering experiences and the research results of the elevation amplification effect of the slope vibration velocity, it is inferred that the mechanism of the elevation effect in the side wall of the underground powerhouse should be similar to that of the slope. The effect of convex geomorphology makes the

amplification effect of the blast stress wave in the vertical direction to be obviously greater than that in the horizontal direction. Therefore, the reflection superposition of the blast stress wave caused by the convex part of the rock anchor beam and the “whiplash effect” of the step part of the rock anchor beam should be the main factors that cause the elevation amplification effect of the blast stress wave in the

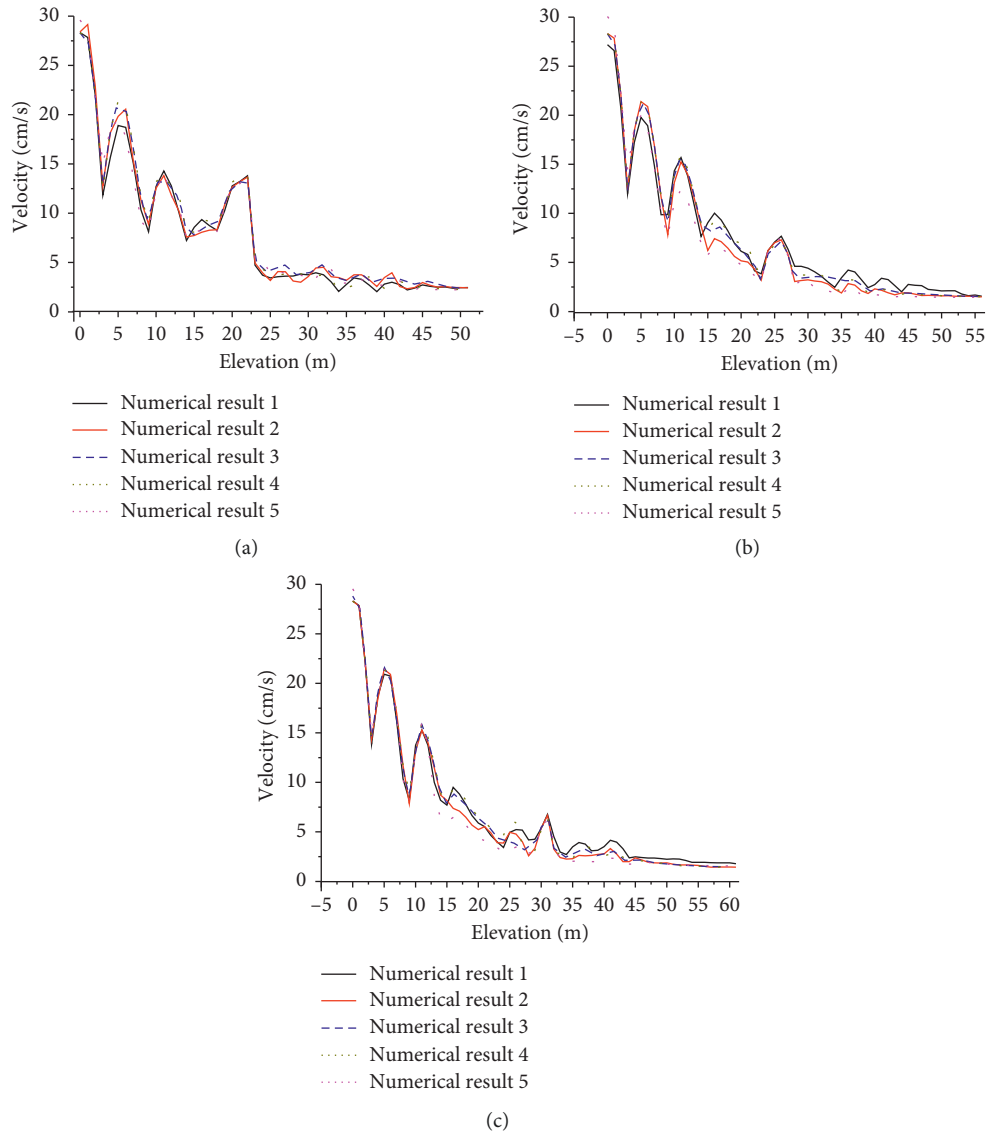


FIGURE 8: Vibration velocity curve of numerical simulation in the elevation direction for layered excavation of the powerhouse. The excavation vibration velocity curve with a horizontal distance of 0 m for (a) the first layer, (b) the second layer, and (c) the third layer.

side wall of the underground powerhouse. The reflection superposition of the convex geomorphology of the rock anchor beam to the blast wave will increase the fluctuation of the propagation process, and the peak position in the fluctuation process is the overlap of the incident wave peak and the reflection wave peak.

In order to explore the influence of the convex geomorphology of the rock anchor beam on the elevation effect of the blast stress wave propagation in the side wall, a new numerical simulation model is established. The simulated working condition is the blasting excavation process for the first layer of the baseboard of the powerhouse, which is divided into five blocks, and a total of five models are established. The mechanical characteristics and blasting parameters needed for numerical simulation are completely consistent with the original excavation model of the first layer, as shown in Figure 11(a). The geomorphological feature of the rock anchor beam is the only variable. The

original numerical model has an outwardly convex geomorphology feature at the rock anchor beam. The new model sets the shape of the side wall as the flat landform before the step part of rock anchor beam is casted, as shown in Figure 11(b). A line of elevation measuring points which are directly above each simulated excavation block and with a horizontal distance of 0 m from the blast source and a height difference of 1 m are selected as objects. There are 52 measuring points. The blast vibration velocity values in the elevation direction of each measuring point are extracted and processed into a graph, as shown in Figure 12.

By controlling the unique variable of the shape characteristics of the rock anchor beam, the corresponding numerical calculation results are analyzed and compared, and the conclusions are obtained as follows. (1) After the rock anchor beam is casted, the vibration velocity of the particles increases from small to large, especially in the rock anchor beam, which is consistent with the measured data laws. (2)

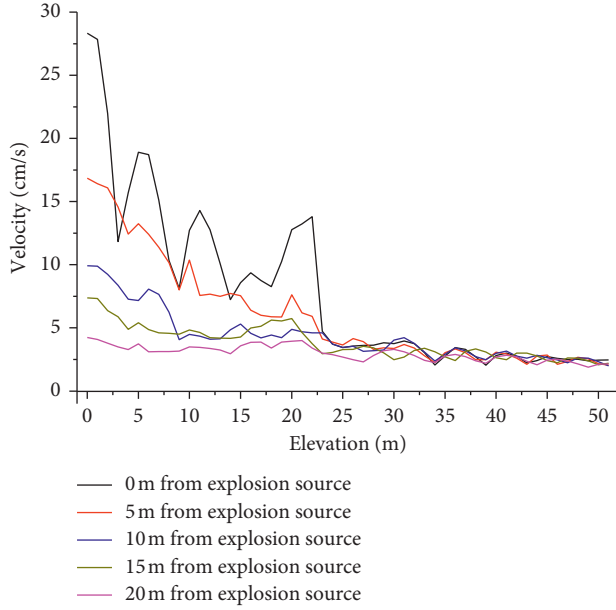


FIGURE 9: Vibration velocity curve in the elevation direction with different horizontal distances.

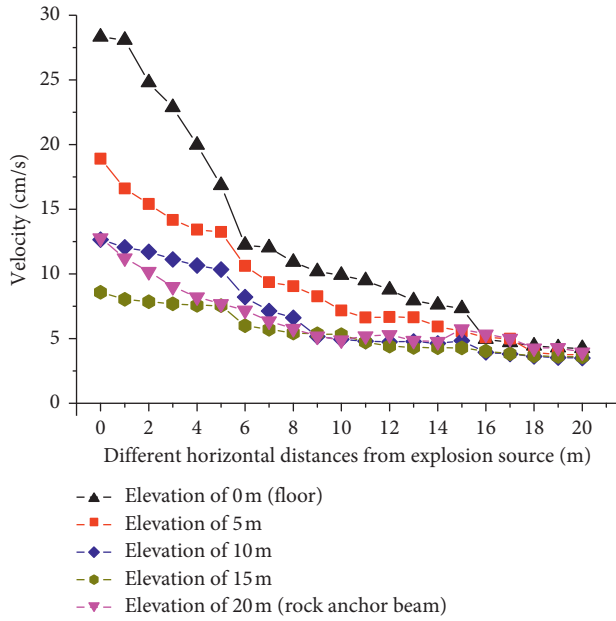


FIGURE 10: Distribution curve of vibration velocity along horizontal distance at different elevations.

The whiplash effect caused by the external convexity of the rock anchor beam exacerbates the elevation amplification effect of the blast wave in the side wall of the powerhouse. The reflection superposition of the convex geomorphology of the rock anchor beam causes the obvious wave propagation phenomenon of the blast wave, and the fluctuation phenomenon of the flat geomorphology of the rock anchor beam is relatively weak. (3) Under the condition of the flat geomorphology of the rock anchor beam, the blasting vibration velocity in the elevation direction also fluctuates slightly. It is analyzed that it should be the result of combination of the

vibration characteristic in the elevation direction of the high side wall of the powerhouse and the reflection superposition of the vault and the baseboard.

4. Mechanism Study of Elevation Amplification Effect

4.1. Generation Mechanism of Elevation Amplification Effect. It is well known that when a building is subjected to an earthquake, if there is a small projecting part on the top of the building, the small projecting part, due to the small mass and stiffness, forms a larger vibration velocity at each moment of turning back and forth, which is called the whiplash effect in the earthquake resistance [18]. For the high side wall of the underground powerhouse, it is a complex structure. In order to study the mechanism of the vibration velocity variation in the elevation direction, it is simplified as a generalized model and a structural vibration computational mechanical model, as shown in Figure 13 [18, 33]. The structure of the step part of the rock anchor beam is equivalent to the projecting part of the main structure of the high side wall. The structural dynamics principle can be used to study the elevation effect of blasting vibration of the high side wall.

As shown in Figure 13, the main body of the high side wall is simplified as the mass point m_1 , and the protrusion of the step part of rock mass at the rock anchor beam is generalized to the mass point m_2 . $y_1(t)$ and $y_2(t)$ are the horizontal displacement functions of particles m_1 and m_2 at the time of t , respectively. k_1 and k_2 are structural stiffness coefficients. $F_1(t)$ and $F_2(t)$ are the time-dependent excitation load functions of the structure.

According to the stiffness method, the structural vibration differential equation is obtained as follows:

$$\begin{cases} m_1 \ddot{y}_1(t) + k_{11}y_1(t) + k_{12}y_2(t) = F_1(t), \\ m_2 \ddot{y}_2(t) + k_{21}y_1(t) + k_{22}y_2(t) = F_2(t). \end{cases} \quad (1)$$

where $\ddot{y}_1(t)$ and $\ddot{y}_2(t)$ are the horizontal acceleration functions of particles m_1 and m_2 at the time of t .

Formula (1) is represented by a matrix as follows:

$$\begin{bmatrix} m_1 \\ m_2 \end{bmatrix} \begin{Bmatrix} \ddot{y}_1 \\ \ddot{y}_2 \end{Bmatrix} + \begin{bmatrix} k_{11} & k_{12} \\ k_{21} & k_{22} \end{bmatrix} \begin{Bmatrix} y_1 \\ y_2 \end{Bmatrix} = \begin{Bmatrix} F_1(t) \\ F_2(t) \end{Bmatrix}. \quad (2)$$

Formula (2) is abbreviated as follows:

$$[M][\ddot{y}] + [K][y] = [F(t)]. \quad (3)$$

where $[K]$ is the stiffness coefficient matrix of the structure and $[M]$ is the mass matrix of the structure.

Under the condition of the harmonic load, that is, $F_j(t) = F_j e^{i\theta t}$ ($j = 1, 2$), the steady-state response of the system is as follows:

$$[y(t)] = \begin{Bmatrix} y_1 \\ y_2 \end{Bmatrix} e^{i\theta t} = [Y]e^{i\theta t}. \quad (4)$$

where $[Y]$ is the particle displacement vector matrix and θ is the dynamic load frequency.

By substituting Formula (4) into Formula (2), we can get the following formula:

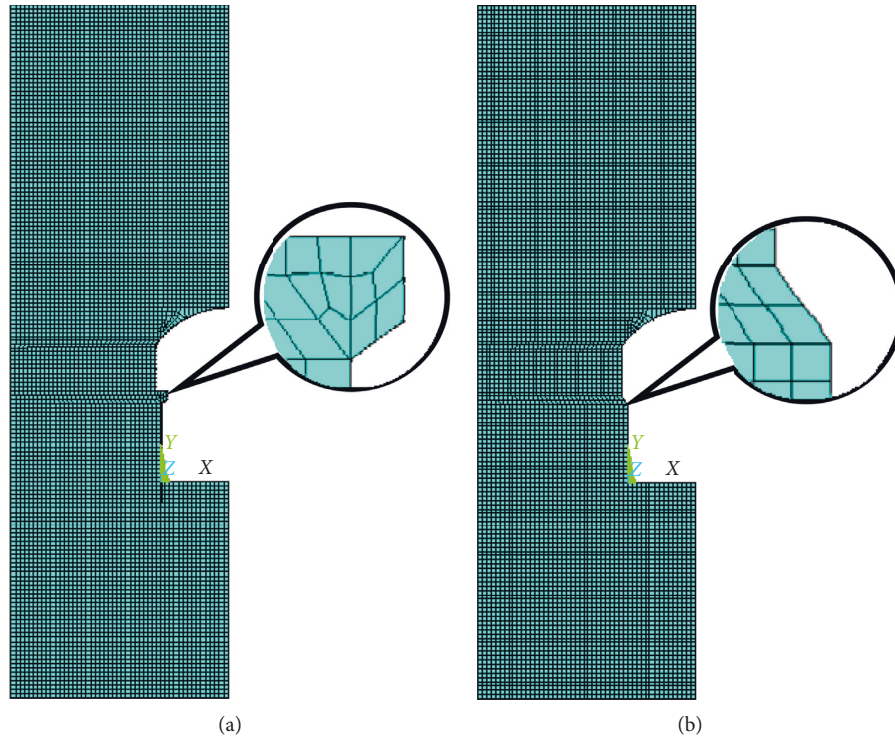


FIGURE 11: Schematic diagram of different morphological characteristics of the rock anchor beam in the numerical model of the underground powerhouse. The model of the rock anchor beam (a) after casting and (b) before casting.

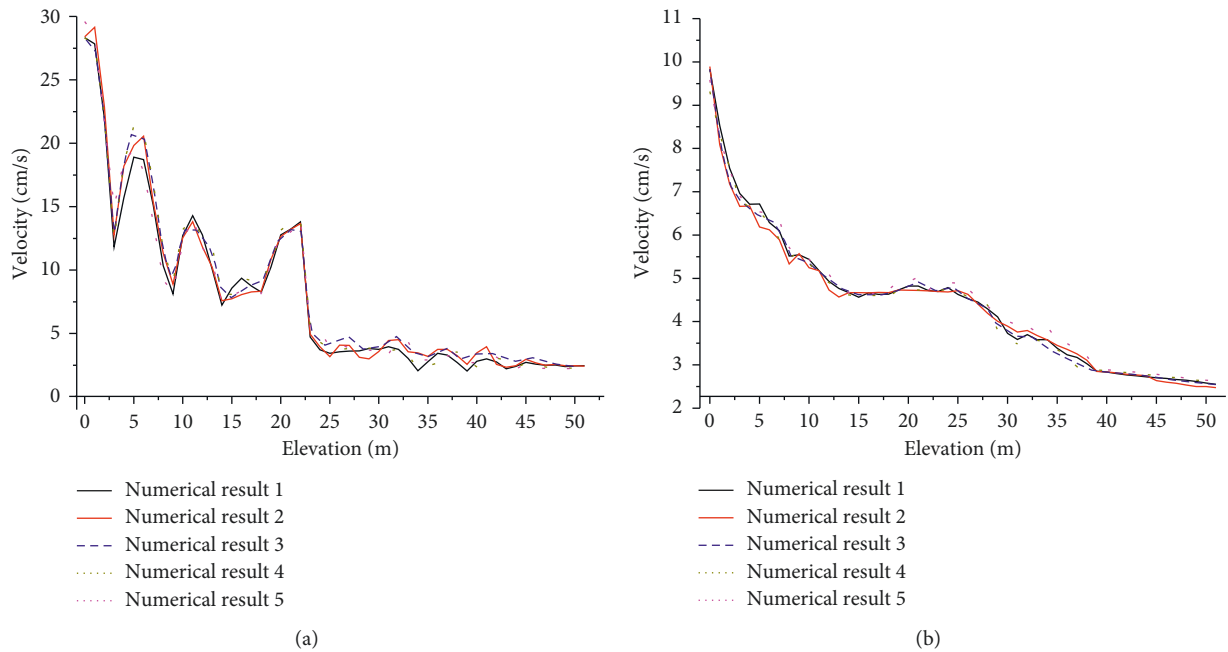


FIGURE 12: Curves of different geomorphology characteristics of the rock anchor beam in the model. Numerical calculation results of the model of the rock anchor beam (a) after casting and (b) before casting.

$$([K] - \theta^2 [M])[Y] = [F]. \quad (5)$$

where $[F]$ is the dynamic load vector matrix of the particle.

According to Formula (5), combined with the boundary conditions of structural vibration, the amplitude $[Y]$ of the

structural vibration can be obtained. Substituting into Formula (4), the vibration displacements at any moment in the structure are obtained. Obviously, when the main frequency θ of the excitation load is equal to the natural vibration frequency ω_2 of the projecting part of the rock

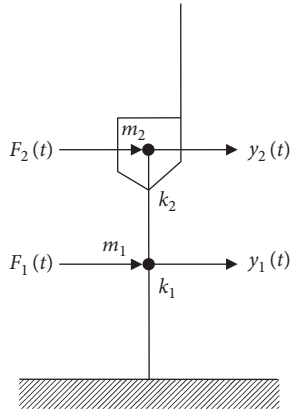


FIGURE 13: Structural vibration computational mechanical model of the high side wall in the underground powerhouse.

anchor beam or the natural vibration frequency ω_1 of the main structure of the side wall, the projecting part will have a vibration amplification phenomenon to form a whiplash effect. According to the test results of blasting vibration, the main frequency of deep hole bench blasting for excavation of high side walls of the underground powerhouse is usually 10 Hz to 300 Hz. If the main natural vibration frequency of the step part of rock mass in the rock anchor beam is in the range of the main frequency band of the blasting vibration load, the vibration response of the step part of the rock mass structure will produce “whiplash effect,” which causes the vibration velocity of rock mass to be amplified. When the shape characteristics of the rock anchor beam, height difference between rock anchor beam and baseboard, surrounding rock lithology, blasting vibration load characteristics, etc., meet certain conditions, the natural vibration frequency of the rock mass in the projecting part of the rock anchor beam is equal to or close to the main frequency of the blasting vibration load. The vibration velocity of the step part of the rock anchor beam may become larger than that of the lower part so that the elevation amplitude amplification effect of the blast vibration is generated.

4.2. Mechanism Study of Wave Propagation Phenomenon of Elevation Magnification Effect. A series of particles on the high side wall that are with the same horizontal distances and different elevations from the blast source are considered as a system of elastic rods perpendicular to the baseboard to discuss the propagation laws in the vibration process. Strictly speaking, the vibration of any elastic structure belongs to the vibration of an infinite degree of freedom system [34]. The so-called infinite degree of freedom system is obtained by infinitely expanding the degree of freedom of a multidegree of freedom system. In the discussion of an infinite degree of freedom system, partial differential equations are needed to be established and complex calculations such as differentiation and integration must be performed. Mathematical derivation is sometimes complicated. It is assumed that the deflection at the time of t caused by the bending is a bending vibration of the $y(x, t)$ rod in its own symmetrical plane, and the dx section microcell is taken along the x direction to conduct force analysis, as shown in Figure 14.

The motion differential equation of the whole rod system can be written as follows.

$$y(x, t) = A \sin \frac{n\pi}{l} x (B \sin \omega t + C \cos \omega t). \quad (6)$$

where A , B , and C are the undetermined coefficients that depend on velocity and displacement.

When $n = 1$, it is the first mode of the system, as shown in Figure 15(a). When $n = 2$, it is the second mode of the system, as shown in Figure 15(b). When $n = 3$, it is the third mode of the system, as shown in Figure 15(c). It can be seen that when a series of measuring points in the elevation direction of the high side wall of an underground powerhouse is generalized into a rod system, the main vibration mode of the fluctuation phenomenon will appear in the propagation process.

It can be seen that when a series of particles in the elevation direction of high side wall is generalized into a horizontally placed rod system, larger amplitude will appear in the middle of the rods of the three vibration modes, and thus the local magnification effect appears in the middle position of the rods. When the second or third vibration mode appears, the vibration of the rod system appears with obvious fluctuation.

5. Conclusion

The following conclusions can be drawn from the comparative analysis of dynamic finite element calculations and field tests and the mechanism study of elevation amplification effects.

An interesting phenomenon is found by analyzing and comparing the blasting vibration velocity values in the elevation direction extracted from a large number of field measured data. The measured vibration velocity of the rock anchor beam in the area far away from the blasting is greater than that in the area near the blasting, and the vibration velocity before the casting of the rock anchor beam is smaller than that after the casting. The same rule has been found by comparing the numerical simulation with the field test. It shows that the blast stress wave has an elevation amplification effect in the propagation process in the side wall of the underground powerhouse, and this amplification effect is generated in the middle of the side wall of the powerhouse, namely, the local part of the rock anchor beam.

The numerical models for two different working conditions of the rock anchor beam before and after casting are established. Based on the comparative analysis of the vibration velocity of the measuring points in the elevation direction at the same location, it is found that the reflection superposition effect of the convex geomorphology characteristics of the rock anchor beam on the stress wave and the whiplash effect of the convex part on the step part of the rock anchor beam are the main reasons for the elevation amplification effect.

By generalizing the side walls of underground powerhouses into elastic rod systems to carry out the mechanism study, it is found that the fluctuation phenomenon of the blast wave in the propagation process of the side wall is

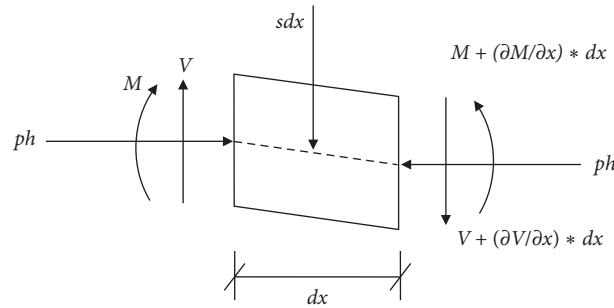


FIGURE 14: Force analysis of microcell.

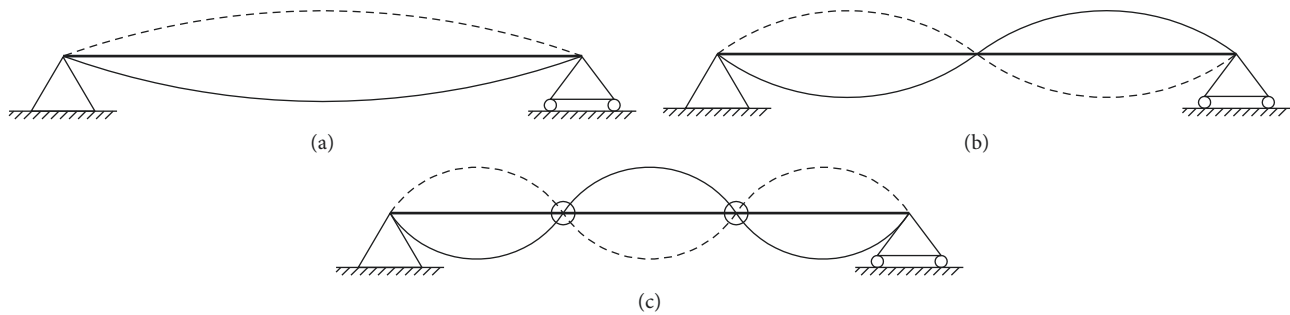


FIGURE 15: The main vibration mode of the rod system. (a) The first vibration mode. (b) The second vibration mode. (c) The third vibration mode.

similar to the main vibration mode produced by the vibration of the rod system. By comparing the calculation results of two numerical models before and after the casting of rock anchor beams, it is found that the reflection superposition of the outwardly convex geomorphology after the casting of the rock anchor beam will aggravate the fluctuation phenomenon of the blast wave in the propagation process, and the peak position in the fluctuation process is the overlap of the incident wave peak and the reflection wave peak.

Due to the limitation of blasting field construction conditions, the measuring points of the blasting vibration test are obviously less than that of the numerical simulation results. The field test only compares and verifies some measuring points of the numerical simulation, and the specific details of the elevation amplification effect are difficult to compare and reflect. In the future, field test research will be continued to carry out in this area.

Data Availability

The data used to support the findings of this study are available from the corresponding author upon request.

Conflicts of Interest

The authors declare that they have no conflicts of interest.

Acknowledgments

The study was supported by “The Fundamental Research Funds for the Chinese Central Universities, China (Grant

No. 2016-YB-024).” The study was supported by “the National Natural Science Foundation of China (Project Nos. 51774222 and 51779197).”

References

- [1] J. H. Yang, W. B. Lu, M. Chen et al., “Microseism induced by transient release of in situ stress during deep rock mass excavation by blasting,” *Rock Mechanics and Rock Engineering*, vol. 46, no. 4, pp. 859–875, 2012.
- [2] S. W. Song, X. M. Chen, B. Y. Xiang et al., “Research on key technologies for high and steep rock slopes of hydropower engineering in southwest China,” *Chinese Journal of Rock Mechanics and Engineering*, vol. 30, no. 1, pp. 1–22, 2011.
- [3] M. Y. Wang, Z. P. Zhou, and Q. H. Qian, “Tectonic, deformation and failure problems of deep rock mass,” *Chinese Journal of Rock Mechanics and Engineering*, vol. 25, no. 3, pp. 448–455, 2006.
- [4] L. X. Xie, W. B. Lu, Q. B. Zhang, Q. H. Jiang, G. H. Wang, and J. Zhao, “Damage evolution mechanisms of rock in deep tunnels induced by cut blasting,” *Tunnelling and Underground Space Technology*, vol. 58, pp. 257–270, 2016.
- [5] L. Ma, K. M. Li, S. S. Xiao et al., “Shu. Research on effects of blast casting vibration and vibration absorption of presplitting blasting in open cast mine,” *Shock and Vibration*, vol. 2016, Article ID 4091732, 9 pages, 2016.
- [6] K. Manoj and S. Mahdi, “A dimensional analysis approach to study blast-induced ground vibration,” *Rock Mechanics and Rock Engineering*, vol. 48, no. 2, pp. 727–735, 2015.
- [7] E. F. Gad, J. L. Wilson, A. J. Moore, and A. B. Richards, “Effects of mine blasting on residential structure,” *Journal of Performance of Constructed Facilities*, vol. 19, no. 3, pp. 222–228, 2005.

- [8] C. Kissinger and I. N. Gupta, "Study of explosion generated dilatational waves in two dimensional models," *Journal of Geophysical Research*, vol. 68, no. 18, pp. 5197–5206, 1963.
- [9] J. E. Field, S. M. Walley, W. G. Proud et al., "Review of experimental techniques for high rate deformation and shock studies," *International Journal of Impact Engineering*, vol. 30, no. 7, pp. 725–775, 2004.
- [10] H. B. Havenith, M. Vanini, and D. Jongmans, "Initiation of earthquake-induced slope failure: influence of topographical and other site specific amplification effects," *Journal of Seismology*, vol. 7, no. 3, pp. 397–412, 2003.
- [11] F. Marrara and P. Suhadolc, "Site amplifications in the city of Benevento (Italy) comparison of observed and estimated ground motion from explosive sources," *Journal of Seismology*, vol. 2, no. 2, pp. 125–143, 1998.
- [12] V. Graizer, "Low-velocity zone and topography as a source of site amplification effect on Tarzana Hill, California," *Soil Dynamics and Earthquake Engineering*, vol. 29, no. 2, pp. 324–332, 2009.
- [13] X. B. Guo, Z. X. Xiao, and Z. C. Zhang, "Slope effect of blasting vibration," *Chinese Journal of Rock Mechanics and Engineering*, vol. 20, no. 1, pp. 83–87, 2001.
- [14] N. Jiang, C. B. Zhou, W. Ping et al., "Latitude effect of blasting vibration velocity in rock slopes," *Journal of Central South University: Science and Technology*, vol. 5, no. 1, pp. 237–243, 2014.
- [15] H. Tang, H. B. Li, P. C. Jiang et al., "Experimental study on the effect of topography on the propagation of blasting wave," *Chinese Journal of Rock Mechanics and Engineering*, vol. 26, no. 9, pp. 1817–1823, 2007.
- [16] H. Tang and H. B. Li, "Study of blasting vibration formula of reflecting amplification effect on elevation," *Rock and Soil Mechanics*, vol. 32, no. 3, pp. 820–824, 2011.
- [17] T. L. Zhou, X. P. Yang, and J. J. Weng, "Experimental study on elevation effect of blasting seism," *Mine Construction Technology*, vol. 12, no. 18, pp. 31–35, 1997.
- [18] M. Chen, W. B. Lu, P. Li et al., "Elevation amplification effect of blasting vibration velocity in rock slope," *Chinese Journal of Rock Mechanics and Engineering*, vol. 30, no. 11, pp. 2189–2195, 2011.
- [19] C. Shi, J. W. Zhou, and Q. Ren, "Ray theory solution of the elevation amplification effect on a single-free-face slope," *Journal of Hehai University (Natural Science)*, vol. 36, no. 2, pp. 238–241, 2008.
- [20] G. M. Song, X. Z. Shi, Z. G. Zhou et al., "Monitoring and assessing method for blasting vibration on open-pit slope in Hainan iron mine," *Journal of Central South University of Technology*, vol. 7, no. 2, pp. 72–74, 2000.
- [21] X. L. Song, J. C. Zhang, X. B. Guo et al., "Influence of blasting on the properties of weak intercalation of a layered rock slope," *International Journal of Minerals, Metallurgy and Materials*, vol. 16, no. 1, pp. 7–11, 2009.
- [22] D. P. Xu, X. T. Feng, Y. J. Cui et al., "Shear behaviors of interlayer staggered zone at Baihetan hydropower station," *Chinese Journal of Rock Mechanics and Engineering*, vol. 31, no. 1, pp. 2692–2703, 2012.
- [23] HydroChina Huadong Engineering Corporation, *Report of Detail Construction Drawing Stage for Excavation and Treatment Measures of Left Dam Spandrel from EL720 m to Riverbed at Baihetan Hydropower Station Along Jinsha River*, HydroChina Huadong Engineering Corporation, Hangzhou, China, 2015.
- [24] G. T. Meng and W. Chu, *Rock Failure Mechanism and Engineering Countermeasures in the Excavation of the First Layer of Baihetan Hydropower Station, Jinsha River*, HydroChina ITASCA R and D Center Corporation Limited, Hangzhou, China, 2014.
- [25] J. X. Lai, H. B. Fan, J. X. Chen, J. L. Qiu, and K. Wang, "Blasting vibration monitoring of undercrossing railway tunnel using wireless sensor network," *International Journal of Distributed Sensor Networks*, vol. 11, no. 6, Article ID 703980, 2015.
- [26] J. Ma, L. F. Luan, and X. H. Li, "Monitoring and analysis of historic building vibration influenced by blasting in complex urban environment," *Applied Mechanics and Materials*, vol. 423, pp. 1558–1562, 2013.
- [27] N. W. Xu, T. Li, and F. Dai, "Stability analysis on the left bank slope of Baihetan hydropower station based on discrete element simulation and microseismic monitoring," *Rock and Soil Mechanics*, vol. 38, no. 8, pp. 2358–2367, 2017.
- [28] M. Saif, W. Wang, A. Pekalski, M. Levin, and M. I. Radulescu, "Chapman-Jouguet deflagrations and their transition to detonation," *Proceedings of the Combustion Institute*, vol. 36, no. 2, pp. 2771–2779, 2015.
- [29] R. Yang, W. F. Bawden, and P. D. Katsabanis, "A new constitutive model for blast damage," *International Journal of Rock Mechanics and Mining Sciences and Geomechanics*, vol. 33, no. 3, pp. 245–254, 1996.
- [30] X. P. Li, J. H. Huang, Y. Luo et al., "Numerical simulation of blast vibration and crack forming effect of rock-anchored beam excavation in deep underground caverns," *Shock and Vibration*, vol. 2017, Article ID 1812080, 13 pages, 2017.
- [31] J. Shi, C. W. W. Ng, and Y. Chen, "Three-dimensional numerical parametric study of the influence of basement excavation on existing tunnel," *Computers and Geotechnics*, vol. 63, pp. 146–158, 2015.
- [32] China's Hydropower Consulting Group, *The Construction Bidding Documents with Civil Engineering and Metal Structure Installation Project on the Right Bank Diversion Generating System of Jinsha River Baihetan Hydropower Station*, China's Hydropower Consulting Group East China Survey Design and Research Institute, Beijing, China, 2013.
- [33] C. W. Yang, J. Y. Zhang, J. Lian, W. Y. Yu, and J. J. Zhang, "Time-frequency analysis method of acceleration amplification along hill slope," *Environmental Earth Sciences*, vol. 75, no. 14, p. 1095, 2016.
- [34] J. F. Xie, "Analysis of the stability of deep slab structure based on the structure resonance induced by the blasting vibration and its application," Master's thesis, Central South University, Changsha, China, 2013.

